Lawrence Berkeley National Laboratory

Title

Cost analysis of distributed storage in AC and DC microgrids

Permalink

https://escholarship.org/uc/item/6sb2t31f

Authors

Gerber, Daniel L
Nordman, Bruce
Brown, Richard
et al.

Publication Date

2023-08-01

DOI

10.1016/j.apenergy.2023.121218

Peer reviewed

Cost Analysis of Distributed Storage in AC and DC Microgrids

Daniel L. Gerber[a,*], Bruce Nordman[a], Richard Brown[a], Jason Poon[b]

[a]*Lawrence Berkeley National Laboratory, Building 90, 1 Cyclotron Rd, Berkeley, CA 94720*
[b]*California Polytechnic State University, 1 Grand Avenue San Luis Obispo, CA 93407*

Abstract

Building and microgrid designs with highly-distributed electrical storage have potential advantages over today's conventional topologies with centralized storage. This paper studies the capital cost benefits of several residential behind-the-meter distributed-storage topologies, including AC and DC versions of systems with load-packaged batteries and resilient sub-networks. The study begins by defining the block configuration of each topology. This work then develops a model for the cost of the power electronics necessary to interface with the storage elements. Finally, the analysis develops a model for the total cost of each storage topology, incorporating the installation and soft costs. The results suggest that while the cost of power electronics is lower in centralized topologies, the total cost is lower for distributed storage due to the avoided costs of installation and permitting. This paper also explores the benefits of load-packaged batteries for savings in electrical infrastructure.

Keywords: battery storage, microgrid, DC power, buildings, soft cost, appliances

1. Background and Motivation

1.1. Motivation for Distributed Storage

Battery storage can provide resilience and allow for peak and time-of-use shifting in buildings and microgrids. Today's storage units range from residential-scale battery packs to commercial-scale battery banks in a shipping container. Most microgrids have a centralized storage topology, in which most of the storage capacity resides at a single physical location. However, some discussions entertain the potential benefits of distributed storage, in which the total storage capacity

---

is partitioned as smaller units and physically distributed throughout the microgrid. These units may be integrated into appliances, deployed as uninterruptible power supplies (UPS) for critical sub-networks, or installed behind solar panels.

The economics of distributed storage is a particularly compelling value proposition. This work is among the first to extensively quantify these capital-cost benefits for several residential topologies. Centralized storage involves labor and soft costs related to installation, engineering, permitting, and safety. In addition, the minimal battery unit is often unaffordable, particularly for customers in disadvantaged communities. On one hand, the material cost of storage scales better in centralized systems due to consolidated power electronics and mechanical enclosures. However, material costs have decreased to the point that they are somewhat comparable with the soft costs of residential deployment [1]. By 2026, the retail cost of lithium-based battery packs (for vehicles) is expected to drop below $100/kWh [2] and the energy density will exceed 0.45 kW/L [3]. Such conditions are economically and physically ideal for the integration and deployment of distributed storage.

Other benefits of distributed storage are related to power capacity and transmission. Some loads (e.g., a cooking range) are only used once per day but have high peak power. These loads require expensive high-gauge wire to support a 30 A circuit. Home electrification will require many such high-power circuits, ultimately forcing the homeowner to undergo a costly panel upgrade [4]. Distributed storage has the potential to smooth power peaks and thus reduce infrastructure requirements. Prior works suggest that localized peak-shaving also allows for savings in wire loss and improvement in overall microgrid stability.

DC microgrids have become relevant due to their compatibility with internally-DC distributed energy resources (DERs) such as solar panels and battery storage. Most modern loads are also internally DC, including electronics, LED lighting, induction cooking, and variable speed drive motors in heat pump HVAC, refrigeration, and water heating. Past research studies the energy and efficiency benefits of DC through modelling [5], simulation [6], and experimentation [7]. Other works attempt to characterize the economic benefits of a fully DC [8] or hybrid DC [9] microgrid building. Some works also examine [10] and reveal [11] the potential power-quality advantages of DC systems. Despite all the potential benefits, adoption of DC has been slow due to a lack of DC site developers and load manufacturers. A significant part of DC research is now to identify adoption pathways and develop a compelling value proposition [12]. As explained in Section 2,

one such proposition is that DC microgrids are highly conducive for distributed storage with bidirectional power flow.

1.2. Prior Work in Distributed Storage

Most prior literature with the term "distributed storage" centers around community or grid-scale assets. This paper specifically studies distributed storage within a residential-scale building. It initiates exploration of a vital research gap: there is currently no prior research that conducts a techno-economic comparison between centralized and distributed storage. Despite this, there is a wealth of literature on related topics that establish a technical background for building-scale distributed storage. This section will review prior related works including storage assets in buildings, optimal asset location, control of distributed storage in AC and DC microgrids, and load-packaged batteries.

There are several successfully deployed examples and use-cases for distributed storage in buildings. The uninterrupted power requirements of data centers often necessitate the use of rack-mounted UPS systems. Studies have shown that distributed control in such systems allows for peak shaving, which can increase battery life [13], allow more servers to operate on a smaller power budget [13, 14], and even provide grid services [15]. Beyond data centers, distributed storage in buildings is uncommon, though present in various pilot projects such as the Shenzhen Institute of Building Research (IBR) DC office building [16]. The IBR building powers local loads through a 48 V power-distribution box. Each box contains a 1 kWh battery, allowing each to form its own resilient DC sub-network: an electrical partition of the building buffered from the main bus by power electronics and storage. Building-level simulations show how such a network topology can benefit power quality [17] and reduce wire transmission loss [18].

The storage capacity and physical location of distributed batteries can greatly affect a microgrid's overall efficiency and life span. Researchers often frame sizing and placement as a optimization problem, which they resolve through various algorithms. For grid-tied systems, prior works study how optimal sizing and placement can improve the bus voltage stabilization [19], system economics [20], and overall network flexibility [21]. For DC microgrids, prior studies highlight power availability [22] and wire loss [18].

For microgrids, most research in distributed storage involves developing controllers for optimal power flow. There are three fundamental levels of control: decentralized primary control within

3

each power converter, distributed secondary control via direct communications between converters, and centralized tertiary control implemented as networked communication with a specialized microgrid controller. For primary control of distributed AC storage, researchers often recommend frequency droop control [23, 24]. Tertiary controllers are demonstrated in AC microgrids through various methods, including optimization-based scheduling [25] and model predictive control [26]. Other works show how optimized peer-to-peer power sharing between distributed storage in multiple buildings can reduce battery size, improve life span, and reduce electricity cost by 3–16% [27]. Such techniques may well be highly applicable to behind-the-meter distributed batteries within a single building and could have a highly positive impact on the economics.

DC microgrid literature contains a wealth of controls research, and many of these prior works study systems with highly-distributed storage assets. These control techniques are showcased in a number of applications, including DC office buildings [16, 17], bipolar microgrids [16, 17, 28], mixed storage applications [29], and rural electrification [30, 31]. Peer-to-peer power sharing within a DC network can improve asset utilization and reduce necessary battery size [22, 32]. For DC microgrids, the most common primary control for storage is voltage droop control [16, 17, 29, 33]. Bus-voltage control, a slow version of droop control, is also popular as a decentralized way to communicate charge or discharge instructions [30]. Previous works have demonstrated battery droop control through various converter topologies, including a non-isolated buck-boost [34] and an isolated dual-active bridge [33]. Secondary control involves direct communication between distributed assets, and relevant literature focuses on state of charge (SOC) balance [35, 36] and minimizing transmission loss [37]. Prior work in tertiary storage control employs methods such as model predictive control [38] and power source virtualization based on SOC [39, 40] to improve microgrid stability and inertia. Some DC research proposes a hierarchical scheme involving all three levels of control [41].

As previously mentioned, distributed storage can be implemented as a load-packaged battery. Although little research involves directly packaging batteries with loads, several prior works study the combination of specific loads with storage assets in microgrid or off-grid applications. Such research can reveal the best practices for efficiently sizing and operating load-packaged storage. For heat pumps applications, relevant research includes cost-optimized sizing strategies [42, 43] and optimization-based model predictive control [44]. Some works even study heat pumps in elec-

tric vehicles for combined space and battery cooling [45]. For induction cooking, most literature applies to small-scale microgrid applications in rural electrification and solar home systems. These works investigate every aspect of the field, including load profile and battery sizing [46], economics [47–49], use cases and market development [50], greenhouse gas impact [49], and cultural and behavioral barriers to adoption [51]. Companies such as Channing Street Copper and Impulse Labs are beginning to commercialize 120 V plug-in induction ranges with a battery to enhance resilience and decrease electrical infrastructure requirements. For lighting-specific microgrids, research applications include stand-alone solar lighting [52], solar home systems [53–55], and street lighting [56, 57]. These works focus on improving LED driver life span [53] and optimizing the power electronics [56, 57], and some even propose the use of a solid-state transformer [54].

1.3. Contributions and Organization

This work investigates the economic value proposition of distributed storage. It examines the capital costs of adding centralized and distributed storage to an AC and DC home. In particular, this work contributes:

- One of the first efforts to benchmark the capital-cost difference between centralized and distributed storage,

- An original analysis and comparison of the capital costs involved in adding behind-the-meter storage to AC and DC residential systems, and

- A novel modelling framework that academics and engineers can use to estimate the capital cost of adding storage and ancillary power electronics to any microgrid system.

The results of this work can fundamentally guide the microgrid, building, battery, and appliance industries in informing how and when distributed storage can be beneficial.

This paper evaluates the economics of distributed storage in several power network topologies. These capital costs to the customer are compared with that of the current benchmark: centralized storage. The analysis includes hard costs such as materials, manufacturing, and installation, and soft costs such as sales, overhead, and profit. All costs are derived explicitly as the incremental cost of adding storage to the current baseline: a home without any storage.

Capital costs of the storage topologies are derived via a bottom-up approach. First, Section 2 defines the characteristics and explains the power-conversion requirements for the AC and DC

centralized and distributed topologies. Section 3 then derives the power converter cost model: a scalable model of the off-the-shelf cost for each type of power converter required in each topology. From these results, Section 4 derives a total-cost model for each topology. The total cost model includes the power converter cost model of Section 3 in addition to the modelled cost of batteries, installation, and all the soft costs required for adding storage to a building. Finally, Section 5 shows how distributed storage has the potential for additional savings in electrical infrastructure.

2. Storage Topologies

This work studies and compares the capital costs of the following microgrid storage topologies:

- **AC-Central**: AC distribution bus with centralized storage (benchmark AC case)

- **DC-Central**: DC distribution bus with centralized storage (benchmark DC case)

- **AC-Load**: AC distribution bus with load-packaged storage

- **DC-Load**: DC distribution bus with load-packaged storage

- **ACAC-Sub**: AC distribution bus with a resilient AC sub-network

- **DCDC-Sub**: DC distribution bus with a resilient DC sub-network

- **ACDC-Sub**: AC distribution bus with a resilient DC sub-network

The structure and defining characteristics of each topology is further explained in Sections 2.1 to 2.3. As previously mentioned, this work studies the incremental cost of adding storage to the baseline case: a home without any storage. Naturally, the AC and DC topology models are respectively cast relative to AC and DC homes, each with the same loads.

AC and DC topologies mainly differ in what types of power converters are needed to interface the distribution bus with storage and loads. In this model, all batteries and loads are internally DC, an assumption previously justified in Section 1.1. AC topologies require AC/DC or DC/AC converters to connect batteries and loads to the distribution bus. DC topologies require DC/DC converters for batteries and some types of loads, while other loads can connect directly to the bus. The modeled AC bus operates at 120/240 V split phase (combined in diagrams for simplicity) and the modelled DC bus operates at 380 V DC.

Another key difference between AC and DC distributed storage is in allowable power flow. Unidirectional storage units can only charge from the microgrid network. Bidirectional storage can both charge and discharge. Bidirectional storage is preferred in distribution networks; its stored energy can power loads anywhere within the microgrid. However, there are several reasons why all of the distributed AC topologies must be unidirectional. First, bidirectional AC converters are difficult to design and only scale well in centralized battery inverters. In contrast, DC converters are easily bidirectional by nature of the circuit topology. DC microgrids also feature a gateway inverter that controls power flow to and from the grid, ensuring batteries will never discharge into the grid. In AC microgrids, the utility generally requires a strict and often arduous interconnection agreement to use bidirectional storage. For example, PG&E allows non-exporting buildings up to two 2-60 second periods of inadvertent export every 24 hours, after which the site would require extensive reverse-power protection [58]. For these reasons, it is currently risky and impractical for highly-distributed storage to be bidirectional in AC networks. Nonetheless, this may well change if distributed storage companies can develop and refine sophisticated zero-export controls and equipment.

The addition of storage as dictated by each topology requires various types of power electronics, shown in Table 1 and explained in Sections 2.1 to 2.3. This study highlights three types of power converters:

- **AC-BiD** - Bidirectional AC/DC or DC/AC inverter

- **AC-UnD** - Unidirectional AC/DC rectifier

- **DC** - Bidirectional DC/DC converter

This work also differentiates how the power converters are added to the system:

- Stand-alone converters such as battery inverters require their own physical enclosure, interconnect, EMI filter, and internal power supplies.

- Integrated converters such as load-packaged rectifiers are often integrated onto an existing printed circuit board and can utilize much of their hosts' hardware. They are denoted by a prime symbol (i.e. AC-BiD', AC-UnD', and DC').

Table 1: Storage Topology Power Electronics Requirements

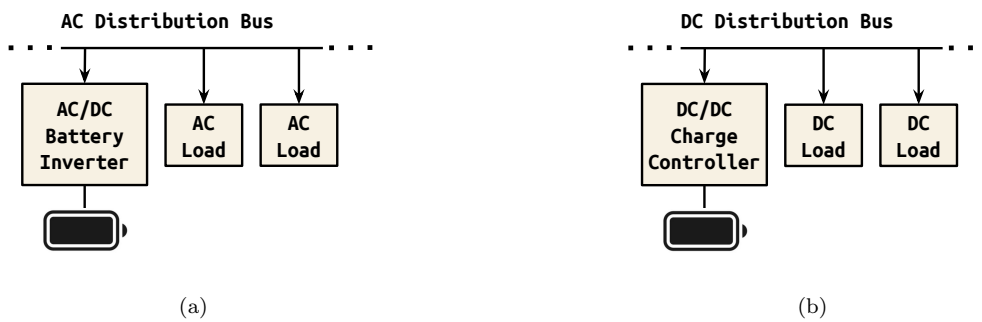| Topology	Converters Required
AC-Central	AC-BiD
DC-Central	DC
AC-Load	60% DC'
DC-Load	DC'
ACAC-Sub	AC-UnD, AC-BiD'
DCDC-Sub	DC
ACDC-Sub	DC

Figure 1: Centralized storage topologies in an (a) AC network and (b) DC network.

On a final note, there are many other methods for connecting distributed storage in a building. Some of these include the use of grid controllers, peer-to-peer power sharing with bilateral contracts, resilient sub-panels, bus stabilizers, and Yotta Energy's practice of packaging batteries behind solar panels. These other topologies are important and promising, but are outside the scope of this paper.

2.1. Centralized Topologies

The benchmark standard for storage is the centralized approach, shown in Figures 1a and 1b for AC and DC systems, respectively. Here, the microgrid storage is consolidated into a single electrical and physical location, often as a battery bank. The battery interfaces with the microgrid network through a single bidirectional converter: a battery inverter in AC systems and a charge controller (CC) for DC.

2.2. Load-Packaged Topologies

Load-packaged distributed storage involves packaging batteries within the physical enclosure of loads. This research develops a model home to assess the cost of load-packaged storage topologies. The home has five resilient loads, each of which has 1 kWh of storage (5 kWh total). These
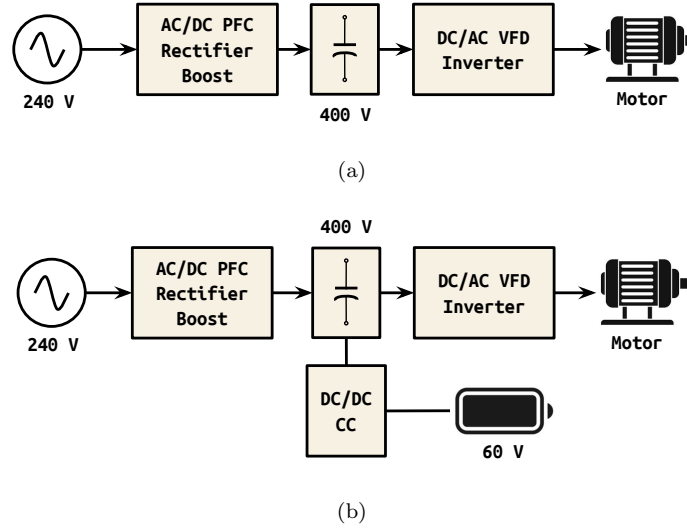
8

Figure 2: AC motor load (mini split compressor) or induction stove coil power electronics block design (a) in common practice today, and (b) with a load-packaged battery.

battery-packaged loads include two mini-split heat pumps, one induction range, and two USB-C hubs. This range of loads covers the most typical modern and future uses for resilience. Heat pumps and induction stoves have long since been established as the future of HVAC and cooking, respectively. While most of today's electronics connect via an AC receptacle, USB-PD 3.1 allows power up to 240 W and 48 V, thus making USB-C a viable plug format for nearly all electronics. USB-C hubs allow for simple plug connections without a wall adapter, and may soon become commonplace for work stations and entertainment centers.

The power-electronics drive train for typical AC motor loads, shown in Figure 2a, includes an AC/DC rectifier capable of power factor correction (PFC), a DC capacitor bus, and a DC/AC variable frequency drive (VFD) inverter. These devices typical use a boost front-end topology with a 350-400 V DC stage. Induction stove drivers have a similar power train structure, and will thus be considered as motor loads for this analysis. As such, 60% of the modelled home's loads are motor loads, and 40% are USB electronics loads.

For AC motor loads, Figure 2b shows that an integrated DC/DC CC is required to add a battery. In general, the DC capacitor stage must be high voltage to generate a sufficient motor drive amplitude and reduce winding loss. While 400 V batteries have become standard in electric vehicles, the need for extensive cell balancing makes them impractical at small capacity. Common 48-60 V battery packs are more realistic for a 1 kWh design.
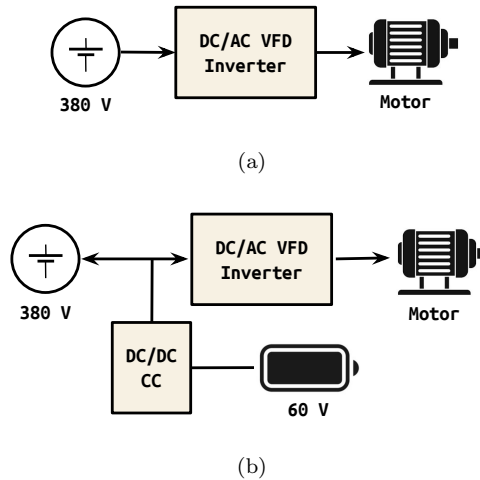
(a)

(b)

Figure 3: DC motor load (mini split compressor) or induction stove coil power electronics block design (a) in common practice today, and (b) with a load-packaged battery.

Figure 3a depicts the drive requirements for a DC motor load, interfaced with an emerging standard 380 V DC bus. DC motor loads only require a VFD inverter [59]. As shown in Figure 3b, adding a battery requires an additional DC/DC CC. This design essentially adds 1 kWh of parallel bidirectional storage to the DC bus, allowing the battery to optionally power other loads in the building. The design can include an input relay if the user wishes only to power the motor load.

AC USB-C electronics, similar to motor loads, have an AC/DC stage and DC capacitor bank. As shown in Figure 4a, PFC rectifier designs may use a boost or flyback topology, with high or low-voltage DC capacitors, respectively. The USB-C output requires a DC/DC converter capable of 5-48 V operation depending on power negotiations with the USB load.

Figure 4b shows how adding a battery to an AC USB-C hub is easier than that of a motor load. Flyback PFC rectifiers can easily output low voltage, depending on the flyback transformer turns ratio. They can also be augmented with a CC algorithm to prevent over-charge. The output DC/DC stage would also require a CC algorithm so as to prevent over-discharge. While 48 V batteries are more common, a 60 V battery guarantees the battery voltage is always higher than the USB-C output, allowing the output stage to use a simple step-down converter.

DC electronics, depicted in Figure 5, just require a single DC/DC converter to interface the 380 V bus with the USB-C load. Adding a battery requires an additional DC/DC CC interface.

In summary, the AC mini-splits and induction range require an additional integrated DC/DC CC (60% of modelled loads) and the USB-C hubs do not. All DC loads require an additional
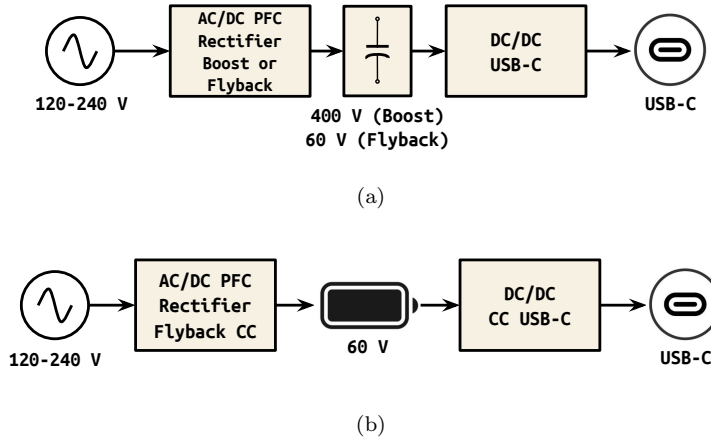
(a)

(b)

Figure 4: AC USB-C hub power electronics block design (a) in common practice today, and (b) with a load-packaged battery.
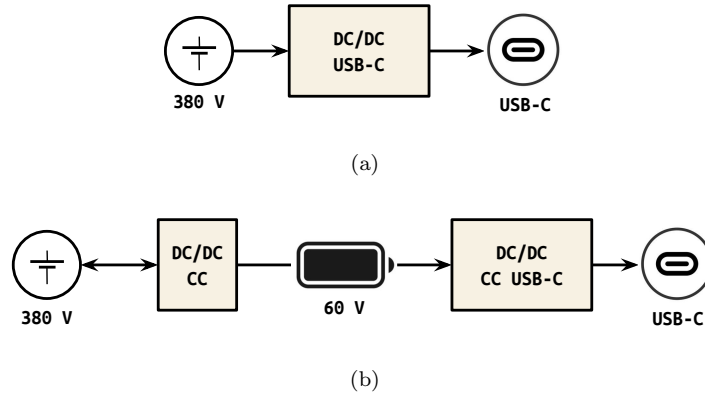

(a)

(b)

Figure 5: DC USB-C hub power electronics block design (a) in common practice today, and (b) with a load-packaged battery.

integrated DC/DC CC. These designs seemingly imply a higher cost of adding storage to DC loads. However, Figures 2 to 5 show that DC loads require fewer conversion stages to begin with. A more comprehensive cost analysis may reveal DC loads with storage to cost less overall, but the scope of this work explicitly targets the incremental cost of adding storage to existing systems.

Finally, note that the DC designs are all bidirectional, allowing load-packaged batteries to power the entire microgrid network. In contrast, AC load-packaged batteries can only power their associated loads. While outside the scope of this study, unidirectional storage will impact the total resilience value of the building. During an outage, occupants may wish to use other loads besides HVAC, cooking, and USB electronics. Such a "lost resilience" cost can be somewhat mitigated through creative design. Mini-splits could include a resilient USB port, powered via a behind-the-wall DC connection to the battery. Induction stoves could include an auxiliary AC receptacle,

11

whose power could be switched over from one of the cook-top inverters during a resiliency scenario. The authors recommend a more meticulous "lost resilience" analysis for future work.

2.3. Resilient Sub-Network Topologies

Resilient sub-networks, shown in Figure 6, are partitions of the microgrid that are buffered from the main bus by power electronics and storage. The power electronics and battery are usually packaged together as a hard-wired or plug-load unit. If hard-wired, these modules are stored behind the wall and act as buffered resilient sub-panels. This study, however, only investigates the plug-load variants. The three topologies differ in their module inputs and outputs.

The most ubiquitous example of an ACAC-Sub network is a UPS. Plug-load examples with relatively high storage capacity include the Orison Panel and Goal Zero Yeti. The ACAC-Sub electronics module requires a 120 V AC-UnD converter at the input and a 120 V AC-BiD for the output (that only operates as an inverter). While the module itself must be stand-alone, one of the two converters can be integrated. Thus the AC-BiD' is integrated into the AC-UnD package.

A common example of an ACDC-Sub network is a resilient Power Over Ethernet (PoE) switch, which has a 120 V AC plug input and multiple point-to-point 48 V DC outputs. These network modules require an AC-UnD input and a DC converter output that regulates the discharge current and PoE channel voltage. Most DC loads on resilient sub-networks are designed to interface directly with the module's DC output, and do not require their own input converter. In the baseline home without storage, these loads would all require their own AC-UnD converter. Thus the assessed converter requirement for ACDC-Sub is only the output DC converter.

DCDC-Sub networks are well-studied in academia but still uncommon in practice. One example of such a network is the power-distribution Box in the IBR DC building [16–18]. The Box has a 380 V DC input and 48 V DC output to office lighting and fans. Similar to the ACDC-Sub topology, the baseline loads would otherwise require their own converters, thus the assessed converter requirement is just the output DC converter of the Box.

On a final note, this work considers USB-C hubs as loads, though one could argue that they are structurally similar to resilient sub-networks. In many ways, a USB-C hub is like a PoE switch. This work assumes that market and industry trends will soon necessitate a USB-C interface for most types of electronics, and thus it establishes USB-C hubs as baseline electronic loads. In contrast, PoE systems are still largely an optional method, which can sometimes be appealing for
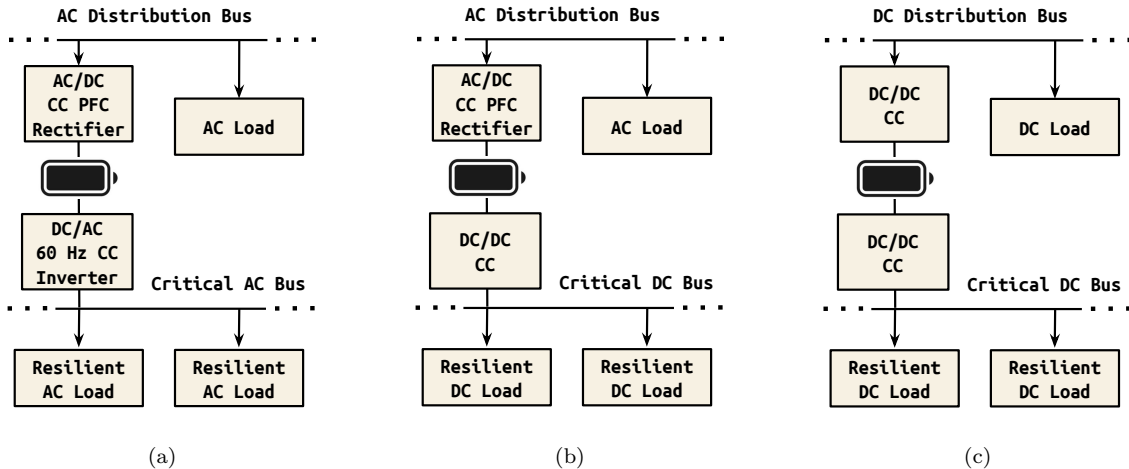
Figure 6: Resilient sub-network topologies under study: (a) ACAC-Sub, (b) DCDC-Sub, and (c) ACDC-Sub transmitting power and data up to 100 m.

3. Power Converter Cost Model

The distributed-storage topologies all differ in the type and scale of power converters they require, as detailed in Table 1. This section describes how the cost of power converters are determined for use in Section 4's total cost model. The analysis method determines the relative material cost of each type of converter, applies a kW scaling curve, and finishes with a cost-category breakdown to determine the Minimum Sustainable Price (MSP) for each converter.

The power converter cost-breakdown model in this study is based on the National Renewable Energy Laboratory (NREL) Inverter model [60]. The NREL Inverter model specifies how to determine the appropriate cost breakdown between materials, manufacturing, selling general and administrative expenses (SG&A), research and development (R&D), and operating margin. This work updates the NREL Inverter model's materials costs to reflect current market value (as of 2022) and scaled production. It assumes the resulting relative breakdown between cost categories can be applied to any AC-BiD battery inverter.

The analysis first determines the relative materials cost of each type of converter: AC-BiD, AC-UnD, and DC. The AC-BiD converter is modeled as an H-bridge inverter in a cascade connected with a flyback dc-dc converter with an active secondary switch (6 MOSFETs). The AC-UnD converter is modeled as a full-wave diode rectifier with a flyback dc-dc converter with a passive secondary switch (1 MOSFET, 5 diodes). The DC converter is modeled as a flyback dc-dc converter

with an active secondary switch (2 MOSFETs).

This work derives the material costs of each converter relative to that of the AC-BiD converter. In the updated NREL AC-BiD Inverter model, the active switching elements (i.e., MOSFETs, including gate drivers and isolated power supplies) comprise 9.03% of the total material costs. Based on cost data scraped from online electronics distributors, the material cost of a passive switch (e.g., a diode for a full-wave rectifier) is approximately 50% the cost of an active switching element. For the updated NREL AC-BiD Inverter, the components related to electromagnetic interference (EMI) filtering comprise 12.3% of the total material costs. Finally, this work assumes that the DC-BiD and DC-UnD converters do not require an EMI filter, since the EMI buffering for these converters is typically achieved with a simple surface-mount capacitor.

As a result, the analysis extrapolates the following materials cost multipliers:

- AC-UnD converters have 93.75% the material cost of AC-BiD converters

- DC converters have 77.72% the materials cost of AC-BiD converters

- Integrated converters have 36.2% the materials cost of stand-alone converters (derived from NREL inverter [60])

This work leverages past data to determine an appropriate scaling curve for the materials cost vs kW capacity of 1-10 kW AC-BiD inverters. References include the updated NREL Inverter model [60] and a previous study on 1-10 kW inverters [61] normalized by battery inverter cost estimates in the NREL 2021 Benchmark Report [1]. Manufacturing costs include assembly and testing labor, energy, utilities, equipment, facilities, and maintenance. They are modelled as a linear interpolation of the sparsely-available manufacturing cost data [60, 62], updated to reflect current (2022) market value. This work assumes 50% manufacturing costs for integrated converters.

This work models the converter cost breakdown as follows:

- Manufacturing - Follows the linear regression: $w = 5.41x + 39.51$, where the manufacturing cost, w, is a function of the kW capacity, x. Assume 50% cost for integrated converters

- Materials - Follows the power regression: $y = 319x^{0.692} - w$, where the materials cost, y, is a function of the kW capacity, x, and the Manufacturing cost, w

- SG&A - 20.3% the sum of Materials and Manufacturing (derived from NREL Inverter [60])
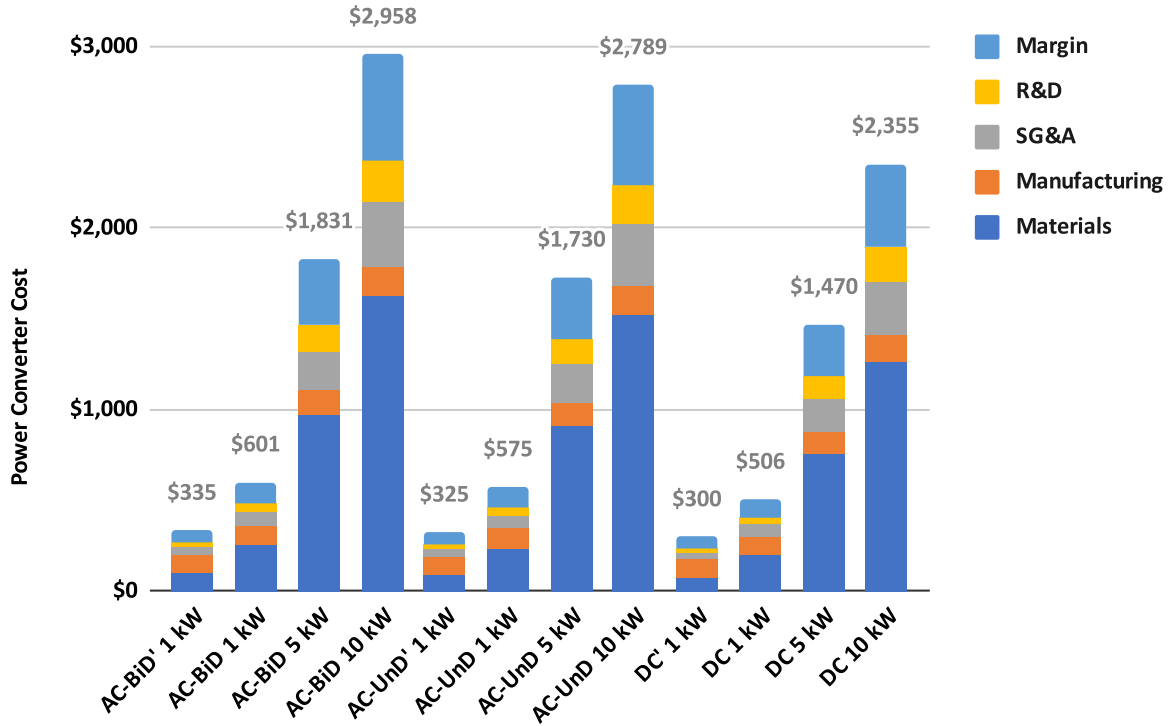
14

Figure 7: Results of the modelled converter cost breakdown including AC-BiD, AC-UnD, and DC topologies sized at 1 kW, 5 kW, and 10 kW. Integrated versions are indicated with a prime (') symbol. Costs are tabulated in Tables A.5 to A.7

- R&D - 13.3% the sum of Materials and Manufacturing (derived from NREL Inverter [60])

- Margin - 32.6% the sum of Materials and Manufacturing (derived from NREL Inverter [60])

The model is applied to integrated and stand-alone AC-BiD, AC-UnD, and DC topologies sized at 1 kW, 5 kW, and 10 kW. The results, shown in Figure 7 are applied directly as the Power Electronics category of the total cost model in Section 4.

4. Total Cost Model

This section analyzes the total costs of installing each storage topology in Section 2. The total cost model is based on the NREL 2021 Benchmark Report [1], with improvements made as appropriate to best represent the differences between topologies. The NREL benchmark model breaks down costs into the following categories: batteries, power electronics, electrical balance of system (BOS) components, supply chain, sales tax, installation labor (burdened), engineering fee, permitting inspection and interconnection, sales and marketing, overhead, and profit margin. The total cost is based on the following category cost models:

- Battery - Priced at $221 per kWh [1]

- Power Electronics - Model derived in Section 3, with kW capacity sized at 50% of the battery kWh capacity for centralized topologies and at 1 kW for distributed

- Electrical BOS - Centralized AC and DC systems both require revenue-grade meters, a communications device, an AC or DC main panel, a DC disconnect, and a sub panel or breaker box [1]. Distributed systems require none (though communications device is optional)

- Supply Chain - 5% of the equipment subtotal (Battery, Power Electronics, Electrical BOS) [1]

- Sales Tax - 6.1% of the equipment subtotal (derived from [1])

- Install Labor - Linearly extrapolated from NREL Benchmark report labor cost data [1] as $31.5x + 908$, where x is the kW capacity of the battery inverter

- Engineering Fee, Permitting, Inspection, and Interconnection (EPII) - Priced at $1765 [1]

- Sales and Marketing - 33% of the direct-cost subtotal (Battery, Power Electronics, Electrical BOS, Supply Chain, Sales Tax, Install Labor, EPII), (derived from [1])

- Overhead - 18% of the direct-cost subtotal (derived from [1])

- Profit - 17% of the sum of all the above cost categories for installers (centralized) [1], 25.8% for wholesalers (distributed) [63]

Distributed-storage topologies allow savings in several of these categories. Since they all involve plug-in battery modules or loads, they can avoid costs associated with Install Labor and EPII. Distributed-storage topologies can also avoid Electrical BOS costs, though could optionally use a $150 communications device to unlock the benefits of bidirectional power flow and flexible load shifting. A final key assumption is that centralized topologies are delivered through an installer, whereas the distributed topologies in this work would be purchased at an appliance wholesaler. For distributed storage, the total cost model aggregates wholesale cost categories of Sales/Marketing, Overhead, and Profit into a single Profit category with a 25.8% margin [63].

The resulting topology comparison of the total cost model is shown in Figures 8 and 9, for total cost and cost-per-kWh, respectively. This study reveals that installation and soft costs of
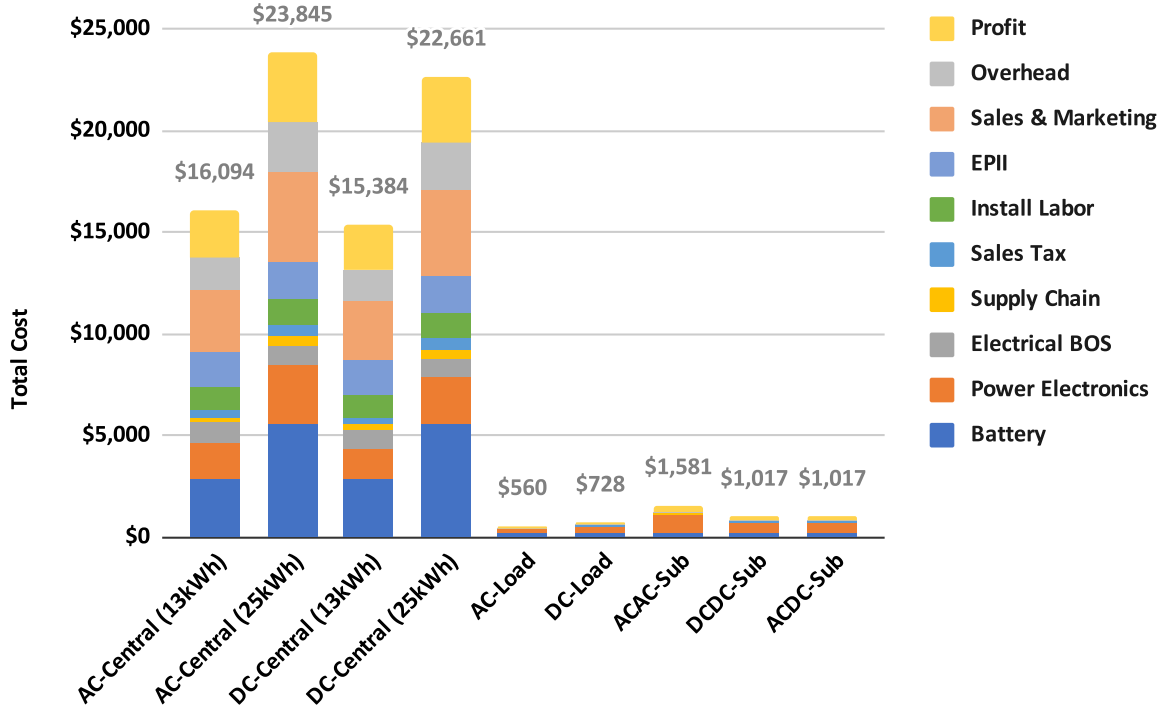
Figure 8: Results of the modelled total cost breakdown of topologies in Section 2. Costs are tabulated in Tables A.8 and A.9

centralized storage can be significant. Overall the AC-Load topology has the lowest cost-per-kWh. As explained in Section 2.2, DC loads often start with fewer power conversion stages, and so the incremental cost of adding storage to DC loads appears higher. Both the AC-Load and DC-Load topologies cost less per kWh than centralized storage. Note that this analysis does not account for costs associated with an increase in the load's footprint and volume due to the addition of batteries.

The resilient sub-networks with DC output have a similar cost-per-kWh as centralized storage. While 25 kWh battery banks cost slightly less, storage at such scale is less common in homes. The more-common 13 kWh centralized systems are more expensive than these DC resilient sub-networks. The ACAC-Sub topology, however, is the most expensive since it requires both a unidirectional and bidirectional AC converter.

5. Load-Packaged Storage Analysis

Of the distributed-storage topologies, unidirectional AC load-packaged batteries may offer the quickest and easiest path to market. This section explains the additional savings potential in
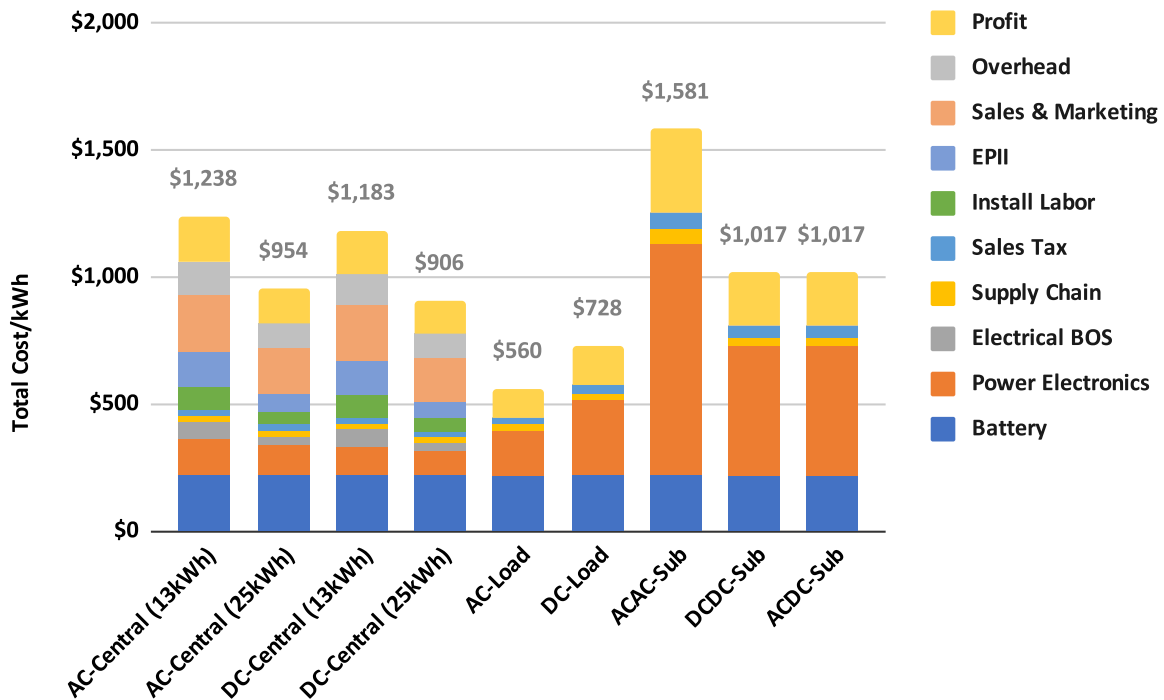
Figure 9: Results of the modelled total cost-per-kWh breakdown of topologies in Section 2. Costs are tabulated in Tables A.10 and A.11

electrical infrastructure and describes sizing requirements for load-packaged batteries.

5.1. Cost of Electrical Infrastructure

In order to meet carbon-emission goals, many homes will have to undergo full electrification, in which they replace existing gas loads with electric equivalents. Common electrification targets include high-power loads such as space heating, water heating, cooking, vehicles, and sometimes clothes dryers. However, electrical versions of these loads often require dedicated 30-50 A circuits and wiring. Full-home electrification can require substantial electrical infrastructure upgrades for the homeowner and utility. For the homeowner, these upgrades include increased wire amperage capacity and panel capacity. The utility may have to upgrade the feeder capacity and even replace a pole-mount transformer.

Distributed storage has the potential to reduce the cost of electrical infrastructure in new construction and retrofits. This work studies how load-packaged storage can reduce the cost of wiring and panel upgrades. It analyzes the savings based on the ability of load-packaged battery to reduce a load's input requirement from 240 V 30 A to 120 V 15 A, making it available as

18

Table 2: NM-B Romex Wire Gauge Amperage and Cost

Gauge (American)	Continuous Amperage	Cost per Linear Foot [64]
10/3	30 A	$2.00
12/3	20 A	$1.27
14/3	15 A	$0.84
12/2	20 A	$0.93
14/2	15 A	$0.63

a NEMA 5-15 plug load. Since infrastructure savings are highly circumstantial, this analysis is excluded from the total cost model in Section 4. Nonetheless, these savings can significantly affect the viability of many retrofits or new constructions.

Wires are sized based on their expected maximum continuous amperage. For new construction, savings can be realized in the wiring cost differential. As shown in Table 2, NM-B Romex wiring for a single-phase 15 A circuit costs significantly less than that of a split-phase (three-wire) 30 A circuit. There may also be further savings opportunities in gas-to-electric load retrofits, particularly if the new electric load can use an existing NEMA 5-15 receptacle, avoiding the labor and material costs of a new wire run.

Panel and service upgrades are another potentially significant cost to homeowners wishing to electrify. Cost data is scarce in academic literature, and past studies have shown a wide variance in actual cost [4]. The total cost (labor and materials) of replacing an electrical panel averages $2,989 over four sources of data. However, up to an additional $10,000 may be required for panel relocation and undergrounding the service drop. These costs are certainly a substantial barrier to mass electrification, especially in disadvantaged urban communities whose homes frequently have low-capacity panels and underground electrical service.

To illustrate the overall infrastructure savings, consider a small single family home with a 100 A panel and service feeder. In this example, a dryer, induction range, two minisplits, and a heat-pump water heater would each require 30 A circuits and 50-foot 10/3 AWG wire runs. Such an influx of 30 A loads would trigger a panel upgrade to 200 A. However, integrated batteries can allow these loads to connect via a 15 A 14/2 AWG circuit. As such, the homeowner can save $2,989 avoiding a panel upgrade and $343 by using 14/2 wire instead of 10/3 wire. In this example, the panel savings are considerably greater than the wire savings, though wire cost can be substantial in retrofits that require running new circuits.

5.2. Battery Sizing for Load-Packaged Storage

Load-packaged batteries only allow for infrastructure savings if the battery is large enough to maintain the load in regular operation. This section studies how to size load-packaged storage to provide resilience or infrastructure savings. Resilience is quantified as the duration (in minutes) by which various loads can maintain normal (or curtailed) operation. The analytic method develops models of typical weekday load profiles that are based on the results of past research [65–68]. While actual usage may vary, these modeled profiles serve to illustrate how to calculate battery capacity requirements for any load. The infrastructure-savings analysis calculates how much load-packaged storage is required to convert a 240 V 30 A appliance to 120 V 15 A. It uses the daily profile, shown in Figure 10. The resilience analysis uses a special resilience-scenario load profile to calculate how many minutes each load can operate from battery power. The loads are modeled as follows:

- The induction range has a small burner, large burner, and oven. The burners run on high for ten minutes, medium for five minutes, and low for ten minutes [65]. The oven preheats for 20 minutes and cycles for an additional 10 minutes. These elements may be initialized simultaneously or offset, in which the small and large burners are activated after 20 and 30 minutes, respectively. In the resilience scenario, the burner pans are replaced every half hour, but the oven retains its temperature after pre-heating.

- The large and small minisplits operate at 240 V 25 A and 120 V 15 A, respectively. The load profile is derived from a heat pump model with a 70°F set point [66], operating during a mild winter. The outdoor temperature is 45.0°F at midnight, drops to 40.3°F at 03:05, and peaks at 59.9°F at 14:15. The resilience scenario profile is identical to the daily profile.

- The dryer operates on normal mode for a 60-minute cycle [65]. The resilience scenario repeats these 60-minute cycles until the battery is drained.

- The heat pump water heater (HPWH) is based on a four-person household weekday model [67]. It activates its backup resistive heating elements when the water temperature dips too low. The resilience scenario assumes the backup heating element is not activated during an outage; the occupant must time their hot-water usage.
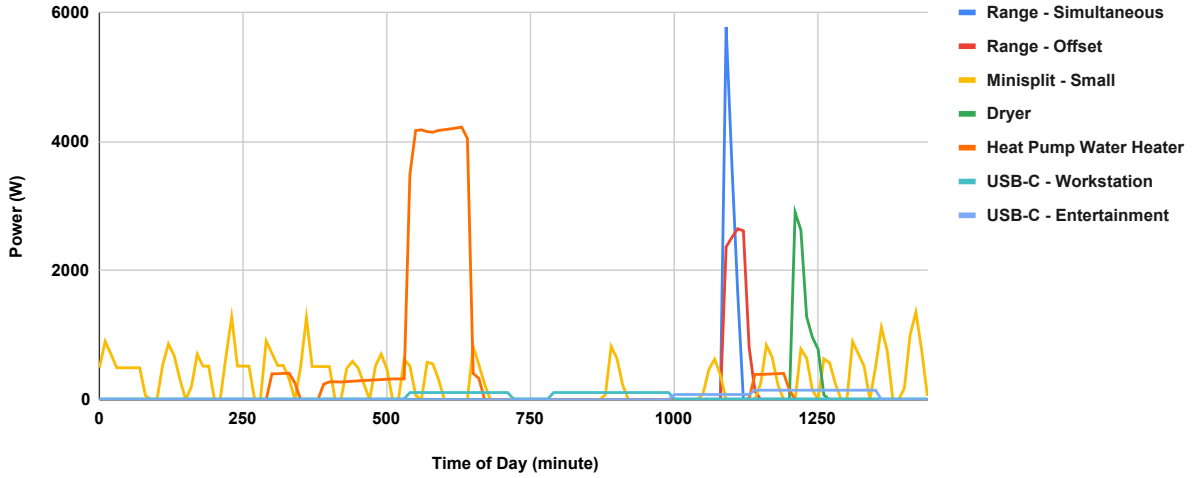
20

Figure 10: Typical load profile models for the infrastructure savings analysis. Load profiles for the resilience analysis are similar, with the differences highlighted in Section 5.2.

Table 3: Battery Capacity for 120 V 15 A Input

Load	Battery (Wh)	Resilience (min)
Range - Simultaneous	1000	10
Range - Offset	500	12
Minisplit Large	900	23
Dryer	400	8
HPWH - Normal Usage	4300	248

- The USB-C workstation powers a desktop computer, monitor, and network gateway [68]. The USB-C entertainment center powers a television and video game console. In both cases, the resilience scenario assumes constant full load.

The results in Tables 3 and 4 are calculated via simulations with 10-minute resolution. Table 3 shows the battery capacity necessary to convert the listed loads from 240 V 30 A to 120 V 15 A. It also shows the minutes of resilience granted by a battery of that size. The large minisplit only needs a 900 Wh battery for a 120 V conversion since its consumption is spread throughout the day. However, the HPWH consumes substantial power in a short period of time; a 120 V conversion would require a large battery. Table 4 shows the minutes of resilience granted to each load for various sizes of integrated battery. Naturally, the storage requirements for electronics are far lower than appliances.

21

Table 4: Battery Capacity for Resilience

Load	1 kWh	2 kWh	3 kWh	4 kWh	5 kWh
Range - Large Burner	40	100	160	220	270
Range - Simultaneous	10	30	40	60	80
Minisplit Large	20	60	120	160	220
Minisplit Small	120	260	380	540	1070
Dryer	20	70	120	140	190
HPWH - HP Only	170	340	510	680	850
USB-C Workstation	530	1060	1590	2120	2650
USB-C Entertainment	400	800	1200	1600	2000

6. Conclusion

The goal of this research is to evaluate the capital cost benefits of distributed storage. This work develops power electronics and total cost models to compare centralized and distributed topologies, including AC and DC versions of systems with load-packaged batteries and resilient sub-networks. The results show that installation and soft costs of centralized storage can be significant. Load-packaged solutions are shown to have the lowest incremental cost of adding storage, as they often already contain the required power converters. Resilient DC sub-networks have an capital cost-per-kWh that is roughly equivalent to that of centralized storage. This paper also describes the potential for further savings if distributed-storage topologies can reduce the need for electrical infrastructure upgrades.

Future work is necessary to further develop the value proposition of distributed storage. The results of this work should be validated by case studies comparing real-world installations. Project data can also reveal the actual savings potential in electrical infrastructure. While this research models capital cost, it lacks an operating-cost assessment, which may affect the results depending on expected equipment life span. A comprehensive techno-economic study could include a sensitivity analysis on various cost components to estimate a future cost breakdown. This work only investigates several distributed storage topologies, but future research may opt to expand the scope of analysis to other emerging topologies such as microgrids with peer-to-peer based sharing and bilateral contracts between distributed batteries. Finally, researchers may want to explore the topic of lost resilience, which may be an issue in buildings with unidirectional load-packaged topologies. AC load-packaged batteries can only power their own specific loads. If researchers can quantify

the cost of lost resilience elsewhere in the building, they may well reveal a major advantage for bidirectional DC topologies.

Acknowledgements

References

[1] V. Ramasamy, D. Feldman, J. Desai, and R. Margolis, "Us solar photovoltaic system and energy storage cost benchmarks: Q1 2021," tech. rep., National Renewable Energy Lab.(NREL), Golden, CO (United States), 2021.

[2] "Lithium-ion battery pack prices rise for first time to an average of \$151/kwh — bloombergnef." `https://about. bnef.com/blog/lithium-ion-battery-pack-prices-rise-for-first-time-to-an-average-of-151-kwh/`. (Accessed on 02/09/2023).

[3] N. Muralidharan, E. C. Self, J. Nanda, and I. Belharouak, "Next-generation cobalt-free cathodes–a prospective solution to the battery industry's cobalt problem," *Transition Metal Oxides for Electrochemical Energy Storage*, pp. 33–53, 2022.

[4] B. D. Less, N. Casquero-Modrego, and I. S. Walker, "Home energy upgrades as a pathway to home decarbonization in the us: A literature review," *Energies*, vol. 15, no. 15, 2022.

[5] A. Othee, J. Cale, A. Santos, S. Frank, D. Zimmerle, O. Ghatpande, G. Duggan, and D. Gerber, "A modeling toolkit for comparing ac vs. dc electrical distribution efficiency in buildings," *SSRN Electronic Journal*, 01 2022.

[6] D. L. Gerber, V. Vossos, W. Feng, C. Marnay, B. Nordman, and R. Brown, "A simulation-based efficiency comparison of ac and dc power distribution networks in commercial buildings," *Applied Energy*, vol. 210, pp. 1167–1187, 2018.

[7] A. Santos, G. Duggan, S. Frank, D. Gerber, and D. Zimmerle, "Endpoint use efficiency comparison for ac and dc power distribution in commercial buildings," *Energies*, vol. 14, no. 18, 2021.

[8] V. Vossos, D. Gerber, Y. Bennani, R. Brown, and C. Marnay, "Techno-economic analysis of dc power distribution in commercial buildings," *Applied Energy*, vol. 230, pp. 663–678, 2018.

[9] C. Charalambous, C. N. Papadimitriou, A. Polycarpou, and V. Efthymiou, "A technoeconomical evaluation of a hybrid ac/dc microgrid Ñ the university of cyprus nanogrid," in *2020 2nd IEEE International Conference on Industrial Electronics for Sustainable Energy Systems (IESES)*, vol. 1, pp. 240–246, 2020.

[10] G. Van den Broeck, J. Stuyts, and J. Driesen, "A critical review of power quality standards and definitions applied to DC microgrids," *Applied Energy*, vol. 229, pp. 281–288, 11 2018.

[11] D. L. Gerber, O. A. Ghatpande, M. Nazir, W. G. B. Heredia, W. Feng, and R. E. Brown, "Energy and power quality measurement for electrical distribution in ac and dc microgrid buildings," *Applied Energy*, vol. 308, p. 118308, 2022.

[12] V. Vossos, D. L. Gerber, M. Gaillet-Tournier, B. Nordman, R. Brown, W. Bernal Heredia, O. Ghatpande, A. Saha, G. Arnold, and S. M. Frank, "Adoption pathways for dc power distribution in buildings," *Energies*, vol. 15, no. 3, 2022.

[13] B. Aksanli, T. Rosing, and E. Pettis, "Distributed battery control for peak power shaving in datacenters," in *2013 International Green Computing Conference Proceedings*, pp. 1–8, 2013.

[14] V. Kontorinis, L. E. Zhang, B. Aksanli, J. Sampson, H. Homayoun, E. Pettis, D. M. Tullsen, and T. Simunic Rosing, "Managing distributed ups energy for effective power capping in data centers," in *2012 39th Annual International Symposium on Computer Architecture (ISCA)*, pp. 488–499, 2012.

[15] B. Zhang and E. N. Senior, "Distributed redundant integration of data center battery storage with the grid for regulation services," in *2021 IEEE Power Energy Society General Meeting (PESGM)*, pp. 1–5, 2021.

[16] J. Kang, B. Hao, Y. Li, H. Lin, and Z. Xue, "The application and development of lvdc buildings in china," *Energies*, vol. 15, no. 19, 2022.

[17] R. Wang, W. Feng, H. Xue, D. Gerber, Y. Li, B. Hao, and Y. Wang, "Simulation and power quality analysis of a loose-coupled bipolar dc microgrid in an office building," *Applied Energy*, vol. 303, p. 117606, 2021.

[18] Y. Bao, W. Feng, H. Xue, R. Brown, B. Nordman, D. Gerber, J. Wang, F. Wang, B. Hao, and Y. Li, "Simulation analysis of commercial-scale direct current building microgrid,"

[19] A. Crossland, D. Jones, and N. Wade, "Planning the location and rating of distributed energy storage in lv networks using a genetic algorithm with simulated annealing," *International Journal of Electrical Power Energy Systems*, vol. 59, pp. 103–110, 2014.

[20] P. Fortenbacher, A. Ulbig, and G. Andersson, "Optimal placement and sizing of distributed battery storage in low voltage grids using receding horizon control strategies," *IEEE Transactions on Power Systems*, vol. 33, no. 3, pp. 2383–2394, 2018.

[21] J. Aghaei, S. A. Bozorgavari, S. Pirouzi, H. Farahmand, and M. Korpås, "Flexibility planning of distributed battery energy storage systems in smart distribution networks," *Iranian Journal of Science and Technology, Transactions of Electrical Engineering*, vol. 44, no. 3, pp. 1105–1121, 2020.

[22] M. Kim, A. Kwasinski, and V. Krishnamurthy, "A storage integrated modular power electronic interface for higher power distribution availability," *IEEE Transactions on Power Electronics*, vol. 30, no. 5, pp. 2645–2659, 2015.

[23] J. Quesada, R. Sebastián, M. Castro, and J. Sainz, "Control of inverters in a low voltage microgrid with distributed battery energy storage. part i: Primary control," *Electric Power Systems Research*, vol. 114, pp. 126–135, 2014.

[24] A. Urtasun, E. L. Barrios, P. Sanchis, and L. Marroyo, "Frequency-based energy-management strategy for stand-alone systems with distributed battery storage," *IEEE Transactions on Power Electronics*, vol. 30, no. 9, pp. 4794–4808, 2015.

[25] C. Abbey and G. Joos, "Coordination of distributed storage with wind energy in a rural distribution system," in *2007 IEEE Industry Applications Annual Meeting*, pp. 1087–1092, 2007.

[26] T. Morstyn, B. Hredzak, R. P. Aguilera, and V. G. Agelidis, "Model predictive control for distributed microgrid battery energy storage systems," *IEEE Transactions on Control Systems Technology*, vol. 26, no. 3, pp. 1107–1114, 2018.

[27] S. M. Ahsan, H. A. Khan, N. ul Hassan, S. M. Arif, and T.-T. Lie, "Optimized power dispatch for solar photovoltaic-storage system with multiple buildings in bilateral contracts," *Applied Energy*, vol. 273, p. 115253, 2020.

[28] H. Kakigano, Y. Miura, T. Ise, and R. Uchida, "Dc micro-grid for super high quality distribution Ñ system configuration and control of distributed generations and energy storage devices," in *2006 37th IEEE Power Electronics Specialists Conference*, pp. 1–7, 2006.

[29] T. Morstyn, B. Hredzak, and V. G. Agelidis, "Cooperative multi-agent control of heterogeneous storage devices distributed in a dc microgrid," *IEEE Transactions on Power Systems*, vol. 31, no. 4, pp. 2974–2986, 2016.

[30] P. A. Madduri, J. Poon, J. Rosa, M. Podolsky, E. A. Brewer, and S. R. Sanders, "Scalable dc microgrids for rural electrification in emerging regions," *IEEE Journal of Emerging and Selected Topics in Power Electronics*, vol. 4, no. 4, pp. 1195–1205, 2016.

[31] D. Zimmerle, A. Felicio B. Santos, and G. P. Duggan, "Dc approximate models for modeling minigrid systems," in *2018 IEEE Global Humanitarian Technology Conference (GHTC)*, pp. 1–7, 2018.

[32] U. G. Mulleriyawage and W. Shen, "Impact of demand side management on peer-to-peer energy trading in a dc microgrid," in *2021 31st Australasian Universities Power Engineering Conference (AUPEC)*, pp. 1–6, 2021.

[33] W. Xing, H. Wang, L. Lu, S. Wang, and M. Ouyang, "An adaptive droop control for distributed battery energy storage systems in microgrids with dab converters," *International Journal of Electrical Power Energy Systems*, vol. 130, p. 106944, 2021.

[34] L. Chen, H. Wu, Y. Xing, and X. Xiao, "Performance evaluation of a 1kw non-isolated high step-up/step-down bidirectional converter for distributed battery storage system," in *2015 IEEE 2nd International Future Energy Electronics Conference (IFEEC)*, pp. 1–5, 2015.

[35] K. D. Hoang and H.-H. Lee, "Accurate power sharing with balanced battery state of charge in distributed dc microgrid," *IEEE Transactions on Industrial Electronics*, vol. 66, no. 3, pp. 1883–1893, 2019.

[36] T. R. Oliveira, W. W. A. Gonalves Silva, and P. F. Donoso-Garcia, "Distributed secondary level control for energy storage management in dc microgrids," *IEEE Transactions on Smart Grid*, vol. 8, no. 6, pp. 2597–2607, 2017.

[37] J. Deng, Y. Mao, and Y. Yang, "Distribution power loss reduction of standalone dc microgrids using adaptive differential evolution-based control for distributed battery systems," *Energies*, vol. 13, no. 9, 2020.

[38] T. Morstyn, B. Hredzak, and V. G. Agelidis, "Dynamic optimal power flow for dc microgrids with distributed battery energy storage systems," in *2016 IEEE Energy Conversion Congress and Exposition (ECCE)*, pp. 1–6, 2016.

[39] N. Piri Yengijeh, H. Moradi CheshmehBeigi, and A. Hajizadeh, "Inertia emulation with the concept of virtual supercapacitor based on soc for distributed storage systems in islanded dc microgrid," *IET Renewable Power Generation*, 2022.

[40] N. Zhi, K. Ding, L. Du, and H. Zhang, "An soc-based virtual dc machine control for distributed storage systems in dc microgrids," *IEEE Transactions on Energy Conversion*, vol. 35, no. 3, pp. 1411–1420, 2020.

[41] J. Zhang, J. T. Csank, and J. F. Soeder, "Hierarchical control of distributed battery energy storage system in a dc microgrid," in *2021 IEEE Fourth International Conference on DC Microgrids (ICDCM)*, pp. 1–8, 2021.

[42] F. Nicoletti, M. A. Cucumo, and N. Arcuri, "Cost optimal sizing of photovoltaic-battery system and airâwater heat pump in the mediterranean area," *Energy Conversion and Management*, vol. 270, p. 116274, 2022.

[43] E. Nordgard-Hansen, N. Kishor, K. Midttomme, V. K. Risinggard, and J. Kocbach, "Case study on optimal design and operation of detached house energy system: Solar, battery, and ground source heat pump," *Applied Energy*, vol. 308, p. 118370, 2022.

[44] R. Gelleschus, M. Bottiger, and T. Bocklisch, "Optimization-based control concept with feed-in and demand peak shaving for a pv battery heat pump heat storage system," *Energies*, vol. 12, no. 11, 2019.

[45] H. Zou, B. Jiang, Q. Wang, C. Tian, and Y. Yan, "Performance analysis of a heat pump air conditioning system coupling with battery cooling for electric vehicles," *Energy Procedia*, vol. 61, pp. 891–894, 2014. International Conference on Applied Energy, ICAE2014.

[46] F. Lombardi, F. Riva, M. Sacchi, and E. Colombo, "Enabling combined access to electricity and clean cooking with pv-microgrids: new evidences from a high-resolution model of cooking loads," *Energy for Sustainable Development*, vol. 49, pp. 78–88, 2019.

[47] O. E. Diemuodeke, M. Orji, C. Ikechukwu, Y. Mulugetta, Y. Sokona, and I. H. Njoku, "Techno-economic analysis of solar e-cooking systems for rural communities in nigeria," in *Advances in Science and Technology*, vol. 107, pp. 203–208, Trans Tech Publ, 2021.

[48] R. Van Buskirk, L. Kachione, G. Robert, R. Kanyerere, C. Gilbert, and J. Majoni, "How to make off-grid solar electric cooking cheaper than wood-based cooking," *Energies*, vol. 14, no. 14, 2021.

[49] F. Antonanzas-Torres, R. Urraca, C. A. C. Guerrero, and J. Blanco-Fernandez, "Solar e-cooking with low-power solar home systems for sub-saharan africa," *Sustainability*, vol. 13, no. 21, 2021.

[50] E. Brown, J. Leary, G. Davies, S. Batchelor, and N. Scott, "ecook: What behavioural challenges await this potentially transformative concept?," *Sustainable Energy Technologies and Assessments*, vol. 22, pp. 106–115, 2017.

[51] S. Batchelor, E. Brown, J. Leary, N. Scott, A. Alsop, and M. Leach, "Solar electric cooking in africa: Where will the transition happen first?," *Energy Research Social Science*, vol. 40, pp. 257–272, 2018.

[52] C.-C. Hua and P.-K. Ku, "Implementation of a stand-alone photovoltaic lighting system with mppt, battery charger and high brightness leds," in *2005 International Conference on Power Electronics and Drives Systems*, vol. 2, pp. 1601–1605, 2005.

[53] B.-J. Huang, C.-W. Chen, P.-C. Hsu, W.-M. Tseng, and M.-S. Wu, "Direct battery-driven solar led lighting using constant-power control," *Solar Energy*, vol. 86, no. 11, pp. 3250–3259, 2012.

[54] S. Liu, X. Zhang, H. Guo, and J. Xie, "Multiport dc/dc converter for stand-alone photovoltaic lighting system with battery storage," in *2010 International Conference on Electrical and Control Engineering*, pp. 3894–3897, 2010.

[55] P. Nair and D. K., "Two-port dc-dc converter with flyback inverter for rural lighting applications," in *2015 International Conference on Technological Advancements in Power and Energy (TAP Energy)*, pp. 249–253, 2015.

[56] K. T. Thanh, H. Yahoui, N. Siauve, N.-Q. Nam, and D. Genon-Catalot, "Construct and control a pv-based independent public led street lighting system with an efficient battery management system based on the power line communication," in *2017 IEEE Second International Conference on DC Microgrids (ICDCM)*, pp. 497–501, 2017.

[57] C.-C. Lin, L.-S. Yang, and E.-C. Chang, "Study of a dc-dc converter for solar led street lighting," in *2013 International Symposium on Next-Generation Electronics*, pp. 461–464, 2013.

[58] "Elec_rules_21.pdf." https://www.pge.com/tariffs/assets/pdf/tariffbook/ELEC_RULES_21.pdf. (Accessed on 02/09/2023).

[59] D. L. Gerber, R. Liou, and R. Brown, "Energy-saving opportunities of direct-dc loads in buildings," *Applied Energy*, vol. 248, pp. 274–287, 2019.

[60] A. Singh, S. Reese, and S. Akar, "Performance and techno-economic evaluation of a three-phase, 50-kw sic-based pv inverter," in *2019 IEEE 46th Photovoltaic Specialists Conference (PVSC)*, pp. 0695–0701, 2019.

[61] N. Abd Rahim, S. Rahman, K. Solangi, M. Othman, and N. Amin, "Survey of grid-connected photovoltaic inverters and related systems," *Clean Technologies and Environmental Policy*, vol. 14, pp. 521–533, 08 2012.

[62] "Pv inverter teardown identifies price-reduction opps." https://www.renewableenergyworld.com/storage/pv-inverter-teardown-identifies-price-reduction-opps/. (Accessed on 02/09/2023).

[63] "Share of gross margin of u.s. electrical goods sales 2017 — statista." https://www.statista.com/statistics/199674/share-of-gross-margin-of-electrical-goods-sales-in-us-wholesale-since-1993/. (Accessed on 02/09/2023).

[64] "Southwire: Pricing." https://www.southwire.com/pricing. (Accessed on 02/09/2023).

[65] M. Pipattanasomporn, M. Kuzlu, S. Rahman, and Y. Teklu, "Load profiles of selected major household appliances and their demand response opportunities," *IEEE Transactions on Smart Grid*, vol. 5, no. 2, pp. 742–750, 2014.

[66] J. Ma, P. Dhillon, W. T. Horton, and J. E. Braun, "Heat-pump control design performance evaluation using load-based testing," 2021.

[67] M. Hoeschele, J. Haile, P. Grant, and K. Cunningham, "Evaluation of unitary heat pump water heaters with load-shifting controls in a shared multi-family configuration," 2022.

[68] B. Urban, K. Roth, and J. Olano, "Energy consumption of consumer electronics in us homes in 2020: Final report to the consumer technology association," *Center for Sustainable Energy Systems Fraunhofer USA: Plymouth, MI, USA*, 2020.

Appendix A. Cost Tables

Table A.5: Power Converter Cost Breakdown (part 1)

	AC-BiD' 1 kW	AC-BiD 1 kW	AC-BiD 5 kW	AC-BiD 10 kW
Materials	$96	$256	$976	$1,629
Manufacturing	$106	$106	$126	$151
SG&A	$41	$73	$224	$361
R&D	$27	$48	$147	$237
Margin	$66	$118	$359	$580
MSP	$335	$601	$1,831	$2,958

Table A.6: Power Converter Cost Breakdown (part 2)

	AC-UnD' 1 kW	AC-UnD 1 kW	AC-UnD 5 kW	AC-UnD 10 kW
Materials	$90	$240	$915	$1,527
Manufacturing	$106	$106	$126	$151
SG&A	$40	$70	$211	$341
R&D	$26	$46	$138	$223
Margin	$64	$113	$339	$547
MSP	$325	$575	$1,730	$2,789

Table A.7: Power Converter Cost Breakdown (part 3)

	DC' 1 kW	DC 1 kW	DC 5 kW	DC 10 kW
Materials	$75	$199	$759	$1,266
Manufacturing	$106	$106	$126	$151
SG&A	$37	$62	$180	$288
R&D	$24	$41	$118	$188
Margin	$59	$99	$288	$462
MSP	$300	$506	$1,470	$2,355

Table A.8: Total Cost Breakdown (part 1)

	AC-Central 13 kWh 6.5 kW	AC-Central 25 kWh 12.5 kW	DC-Central 13 kWh 6.5 kW	DC-Central 25 kWh 12.5 kW
Battery	$2,873	$5,525	$2,873	$5,525
Power Electronics	$1,831	$2,958	$1,470	$2,355
Electrical BOS	$919	$919	$919	$919
Supply Chain	$281	$470	$263	$440
Sales Tax	$343	$574	$321	$537
Install Labor	$1,097	$1,286	$1,097	$1,286
EPII	$1,765	$1,765	$1,765	$1,765
Sales & Marketing	$3,006	$4,454	$2,874	$4,233
Overhead	$1,640	$2,429	$1,567	$2,309
Profit	$2,338	$3,465	$2,235	$3,293
Total	$16,094	$23,845	$15,384	$22,661

Table A.9: Total Cost Breakdown (part 2)

	AC-Load 1 kWh 1 kW	DC-Load 1 kWh 1 kW	ACAC-Sub 1 kWh 1 kW	DCDC-Sub 1 kWh 1 kW	ACDC-Sub 1 kWh 1 kW
Battery	$221	$221	$221	$221	$221
Power Electronics	$180	$300	$910	$506	$506
Electrical BOS	$0	$0	$0	$0	$0
Supply Chain	$20	$26	$57	$36	$36
Sales Tax	$24	$32	$69	$44	$44
Install Labor	$0	$0	$0	$0	$0
EPII	$0	$0	$0	$0	$0
Sales & Marketing	$0	$0	$0	$0	$0
Overhead	$0	$0	$0	$0	$0
Profit	$115	$149	$324	$209	$209
Total	$560	$728	$1,581	$1,017	$1,017

Table A.10: Total Cost/kWh Breakdown (part 1)

	AC-Central 13 kWh 6.5 kW	AC-Central 25 kWh 12.5 kW	DC-Central 13 kWh 6.5 kW	DC-Central 25 kWh 12.5 kW
Battery	$221	$221	$221	$221
Power Electronics	$141	$118	$113	$94
Electrical BOS	$71	$37	$71	$37
Supply Chain	$22	$19	$20	$18
Sales Tax	$26	$23	$25	$21
Install Labor	$84	$51	$84	$51
EPII	$136	$71	$136	$71
Sales & Marketing	$231	$178	$221	$169
Overhead	$126	$97	$121	$92
Profit	$180	$139	$172	$132
Total	$1,238	$954	$1,183	$906

Table A.11: Total Cost/kWh Breakdown (part 2)

	AC-Load 1 kWh 1 kW	DC-Load 1 kWh 1 kW	ACAC-Sub 1 kWh 1 kW	DCDC-Sub 1 kWh 1 kW	ACDC-Sub 1 kWh 1 kW
Battery	$221	$221	$221	$221	$221
Power Electronics	$180	$300	$910	$506	$506
Electrical BOS	$0	$0	$0	$0	$0
Supply Chain	$20	$26	$57	$36	$36
Sales Tax	$24	$32	$69	$44	$44
Install Labor	$0	$0	$0	$0	$0
EPII	$0	$0	$0	$0	$0
Sales & Marketing	$0	$0	$0	$0	$0
Overhead	$0	$0	$0	$0	$0
Profit	$115	$149	$324	$209	$209
Total	$560	$728	$1,581	$1,017	$1,017